

https://doi.org/10.1070/QEL17639

Experimental study of a 100-W all-fibre amplifier operating near 980 nm

M. Chen, H. Du, J. Cao, A. Liu, Zh. Pan, Zh. Huang, J. Chen

Abstract. **A 100-W all-fibre amplifier operating near 980 nm is demonstrated with a double-clad Yb-doped fibre (DCYF) having a 60/125-μm core/cladding diameter. By preliminarily optimising the length of DCYF (about 1.4 m), a total output power of about 113.4 W is obtained with 9-W seed light, the peak-to-peak suppression of 1030-nm ASE being about 21.5 dB. The effect of active fibre length is studied using the experimental setup. With the help of spectrum integration, it is found that while the total output power decreases, the output power around 980 nm is enlarged with the active fibre (i.e., DCYF) further shortened to 1.2 m, which is due to better suppression of 1030-nm ASE. It means that the effect of 1030-nm ASE cannot be simply neglected when its peak-to-peak suppression is lower than 30 dB. The effect of seed power on the output properties of the amplifier is also studied experimentally. It is found that a stronger seed power is beneficial to the 1030-nm ASE suppression and slope efficiency improvement. Then, with the 1.2-m DCYF and 14-W seed power, the largest output signal power around 980 nm (estimated about 108.2 W) is eventually obtained and the peak-to-peak suppression of 1030-nm ASE is more than 33 dB at the maximum output power. The pertinent results can provide significant guidance for the design and study of a 980-nm laser and other sorts of three-level fibre laser.**

Keywords: *laser amplifiers, fibre, ytterbium, amplified spontaneous emission.*

1. Introduction

High-power Yb-doped fibre lasers and amplifiers operating near 980 nm have drawn much attention because of their potential applications as a pump source of high-power Yb/Er-doped fibre lasers and other novel sources such as the blue and ultraviolet sources [1–6].

However, compared with the Yb-doped fibre laser at a longer wavelength (generally longer than 1030 nm), it is challenging to produce high-power 980-nm lasing [2, 7–11]. On the one hand, according to the energy-level of the Yb ion [2], the emission near 980 nm is produced by the three-level transmission of the Yb ion (more than 50% Yb-ion population inversion is needed), while the emission at a longer wavelength is produced by the four-level transmission of the Yb ion (more than 5% population inversion is needed). Therefore, it leads to a higher pump threshold of the emission near 980 nm and serious gain competition between the emissions near 980 nm and the longer wavelength. On the other hand, it is very difficult to make the emission near 980 nm dominant in the gain competition because of the large absorption cross section of the Yb-doped fibre near 980 nm (much larger than that at a longer wavelength [8]), resulting in serious re-absorption of emission near 980 nm. Moreover, it should be noted that the re-absorbed emission near 980 nm can also be used to produce the emission at a longer wavelength, which makes the amplification of emission near 980 nm more difficult.

Fortunately, Jelger et al. [7] revealed that the 980-nm emission can be dominant in the gain competition with the 1030-nm ASE as long as the core-to-cladding ratio is large enough, with the guidance of which various types of Yb-doped fibres were designed and tested, e.g., the air-jacket ring-doped fibre [12], rod-type photonic crystal fibre (PCF) [13, 14], tapered large-core fibre [15], saddle-shaped fibre [16], all-solid photonic bandgap fibre (PBF) [17–21], and so on. The first 100-W-level lasing around 980 nm was obtained from a fibre oscillator fabricated with the rod-type PCF. In this scheme, the 80/200-μm core/cladding-diameter rod-type Yb-doped PCF was used to suppress the 1030-nm ASE, and 94-W near-diffraction-limited output beam was obtained eventually with the slope efficiency of 48% [13]. However, because of the large core of the PCF, the bulk optics scheme involving the spatial light coupling was used in the system [13, 14], which made the whole system less robust and portable. Later, in 2019, a 151-W all-fibre oscillator operating near 980 nm was demonstrated with the all-solid PBF [21]. By inducing high loss in the band of 1030-nm ASE in the PBF, sufficient suppression of 1030-nm ASE was realised with about 21/124-μm core/cladding diameter. As a result, the 151-W near-diffraction-limited output beam was obtained with the slope efficiency of 63%.

Besides the fibre oscillator, the fibre amplifier operating near 980 nm also draws attention because of its important role in the power scalability of fibre lasers. In 2017, Aleshkina et al. [22] demonstrated a 34-W all-fibre amplifier with a double-clad Yb-doped fibre (DCYF) having a 95/125-μm core/cladding diameter and a slope efficiency of 66% [22]. Although the super-large core of the active fibre bring difficulty in the beam quality controlling, it is still attractive in the applications with a lower requirement of the beam quality (e.g., as a tandem pump source of rear-earth-doped fibre lasers [1]). In

M. Chen, H. Du, J. Cao, A. Liu, Zh. Pan, Zh. Huang, J. Chen College of Advanced Interdisciplinary Studies, National University of Defense Technology, Changsha, 410073, China; State Key Laboratory of Pulsed Power Laser Technology, Changsha, 410073, China; Hunan Provincial Key Laboratory of High Energy Laser Technology, Changsha, 410073, China;
e-mail: jq_cao@126.com; cmn2015310162@163.com; 17673122794@163.com; panzy168@163.com; hzhihe@163.com; kdchenjinbao@aliyun.com

Received 25 May 2021; revision received 30 August 2021
Kvantovaya Elektronika **51** (11) 976–982 (2021)
Submitted in English

2020, a 39-W all-fibre amplifier with a near-diffraction-limited beam quality was also presented with a W-profile fibre [23]. However, because of the small core-to-cladding ratio (35/125) of the active fibre, only 19% slope efficiency was obtained. While numerical studies have revealed that the 100-W-level 980-nm fibre amplifier can be realised with a large-core DCYF [24, 25], the pertinent experimental study is very rare.

Thus, in this paper, a 100-W all-fibre amplifier operating near 980 nm is demonstrated with a 60/125-µm core/cladding-diameter DCYF. By using a bi-directional pumping scheme, more than 100-W output power can be obtained. The amplifier is tested with an all-fibre oscillator operating near 980 nm as a seed source. The effects of active fibre length and seed power on the output properties of the amplifier are also investigated in experiment.

2. Experimental setup

The experimental setup of the all-fibre amplifier is shown in Fig. 1. Here, the DCYF with the 60/125-µm core/inner-cladding diameter is utilised as the active fibre, and the numerical aperture (NA) of the inner cladding and the core of the active fibre are 0.46 and 0.1, respectively. Such a DCYF is adopted, because it can provide a large core-to-cladding ratio to suppress the 1030-nm ASE [25]. Besides, the inner cladding of the DCYF is octagonal, which is used to increase the cladding pump absorption efficiency, and its absorption is about 6.8 dB m^{-1} at 915 nm. The DCYF should also be photo-darkening free. By using two side-pumping combiners, the bi-directional pump scheme is realised in our experiment in order to obtain a high pump power. Then, four pig-tailed 915-nm laser diodes (LDs) are used as pump sources, and totally 307-W pump light can be injected into the active fibre through the two side-pumping combiners. The cladding light stripper (CLS) is used to filter out the residual pump light. Besides, the signal light is coupled out through an endcap.

In order to test the amplifier, an all-fibre oscillator near 980 nm is utilised as a seed source (the configuration is similar to that is Ref. [26]). The seed source consists of four pig-tailed 915-nm LDs, two (2 + 1) × 1 fibre combiners, a 0.46-m length DCYF, a high-reflectivity fibre Bragg grating (HR FBG), a low-reflectivity fibre Bragg grating (LR FBG), two CLSs, a band-passing filter, and a mode field adaptor (MFA). Four 915-nm LDs are used as pump sources of the oscillator, and two FBGs with centre wavelength of around 978 nm form the cavity of the oscillator. Here, the HR FBG has the central reflectivity of around 99.5% and the bandwidth of around 2 nm, while the LR FBG has the central reflectivity of around 15% and the bandwidth of around 0.5 nm. A 0.46-m long 20/125-µm DCYF is used as an active fibre, and two CLSs are used to remove the residual pump light. The bandpass filter is employed not only to filter out the 1030-nm ASE produced in the oscillator, but also to protect the seed from any feedback of the amplifier.

Then, the seed light can be injected into the amplifier through the MFA, and the output power and spectrum of the seed light after the MFA are measured (Fig. 2). It can be seen that the seed power increases linearly with pump power. One can see from Fig. 2b that there are two peaks in the output spectrum of the seed light, which are around 977.6 nm and 978 nm, respectively. The two-peak pattern is induced by the reflection spectra of LR and HR FBGs. In spite of that, the seed light is all located within the wavelength range from 977 nm to 978.6 nm, and no ASE around 1030 nm can be observed.

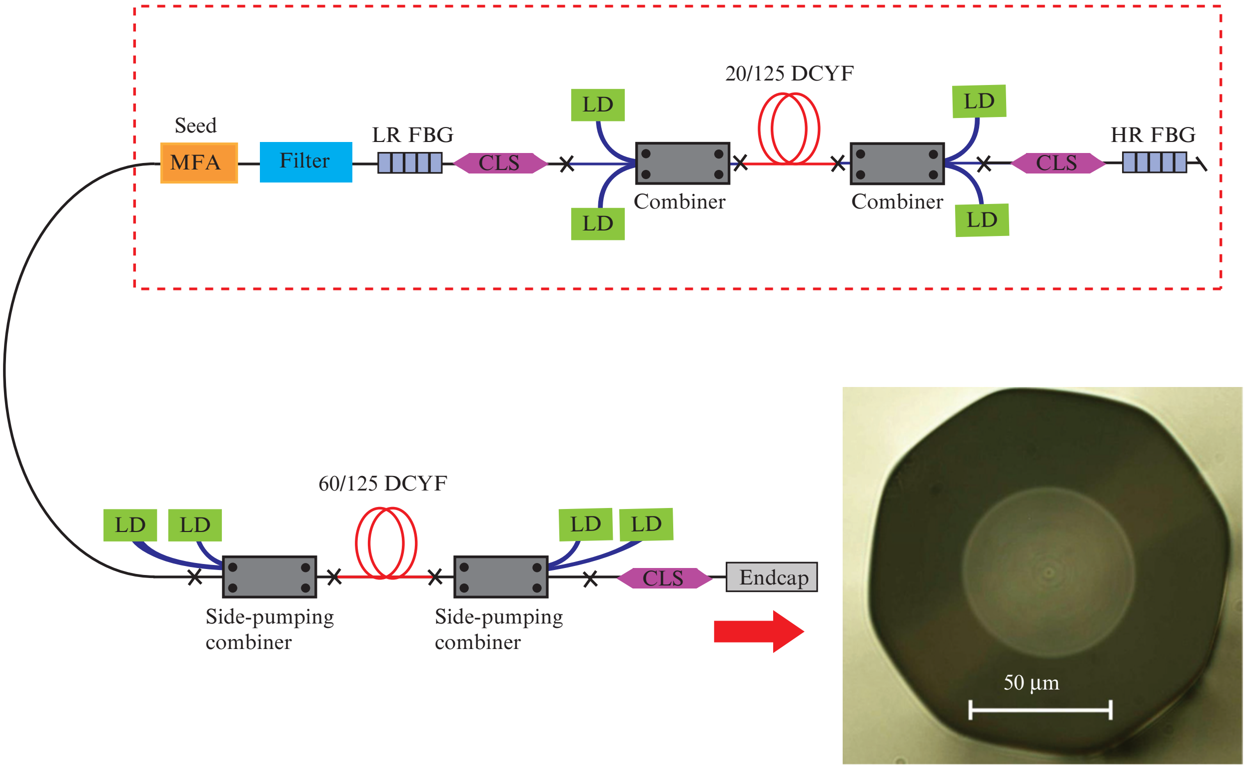

Figure 1. (Colour online) Experimental setup of the 980-nm all-fibre amplifier (the inset shows the image of the 60/125-µm DCYF).

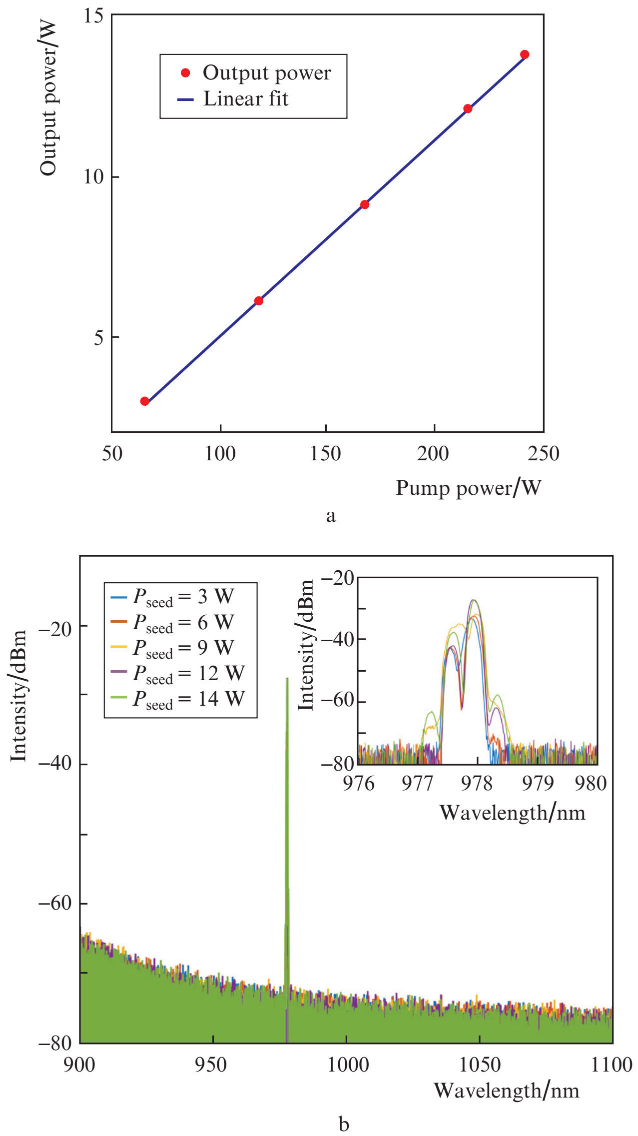

Figure 2. (Colour online) (a) Output power and (b) spectrum of the seed light after the MFA (the inset shows zoom-in spectra around 980 nm).

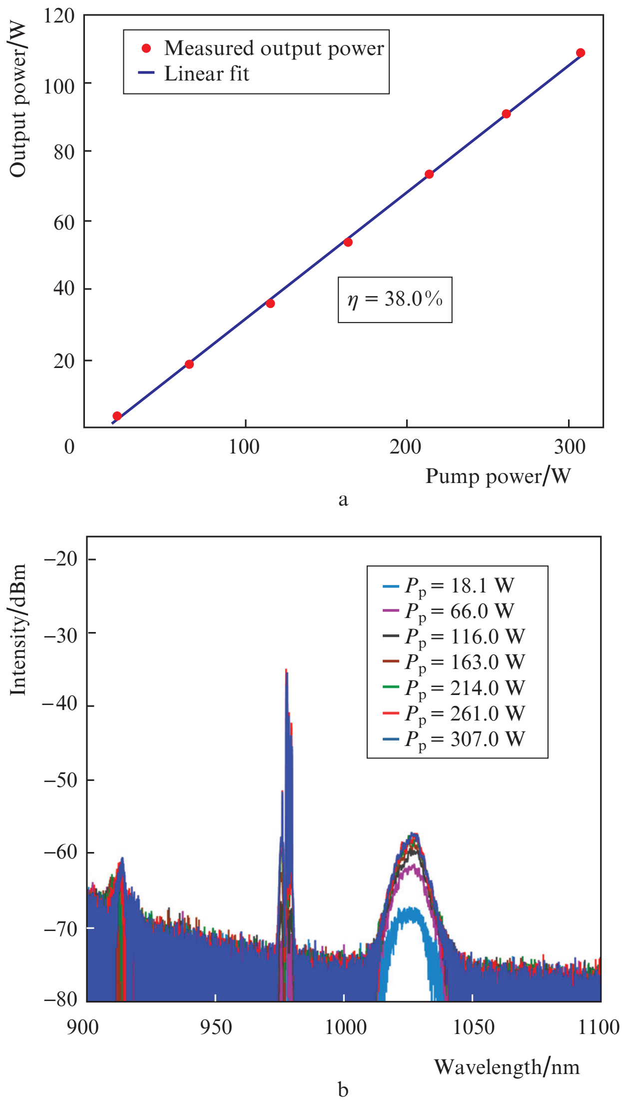

Figure 3. (Colour online) Dependences of (a) measured output power and (b) spectrum on the pump power P_p.

3. Experimental results and discussions

3.1. Effect of active fibre length

Former studies have revealed that the active fibre length is of great importance for the 1030-nm ASE suppression in the 980-nm Yb-doped fibre source [10, 11, 24–26]. With a long active fibre, the serious 1030-nm ASE will be induced and the 980-nm emission will be suppressed [25, 26]. Therefore, the effects of active fibre length on the output properties of the amplifier are studied, firstly. Here, the 9-W seed power is used. By means of gradually shortening the active fibre, we found that the 1030-nm ASE can be suppressed when the active fibre is shortened to 1.4 m. The measured output power and spectrum (Fig. 3) demonstrate that the output power increases linearly with pump power, and 113.4-W output power is eventually obtained with the 307-W pump power and the slope efficiency η is about 38%. It follows from Fig. 3b that 21.5-dB suppression of 1030-nm ASE is realised at a maximum output power.

To study the effect of active fibre length, we further shortened the active fibre and measured the output properties. Figure 4 shows the variations of the output power and spectrum of the amplifier with the 1.3-m and 1.2-m active fibre. From Fig. 4a, it can be seen that when the active fibre is shorted to 1.3 m, the 37% slope efficiency is obtained and 111.3-W output power is eventually realised with the 307-W pump power. Figure 4b also demonstrates that the 26-dB peak-to-peak suppression of 1030-nm can be realised at a maximum output power. When the active fibre is shortened to 1.2 m, the slope efficiency becomes 36.5% and 110-W output power is obtained (see Fig. 4c). Figure 4d shows that the peak-to-peak suppression of 1030-nm ASE increases to 32 dB at the 110-W output power. By comparing these results with the case of 1.4-m active fibre (see Fig. 3), it can be found that there are two effects caused by the shortening of active fibre length. The first one is the reduction of the slope efficiency of the output power, which should be induced by the lower pump absorption owing to the active fibre shortening. The second one is the better suppression of 1030-nm ASE induced by the shorter active fibre [10, 11, 24–26].

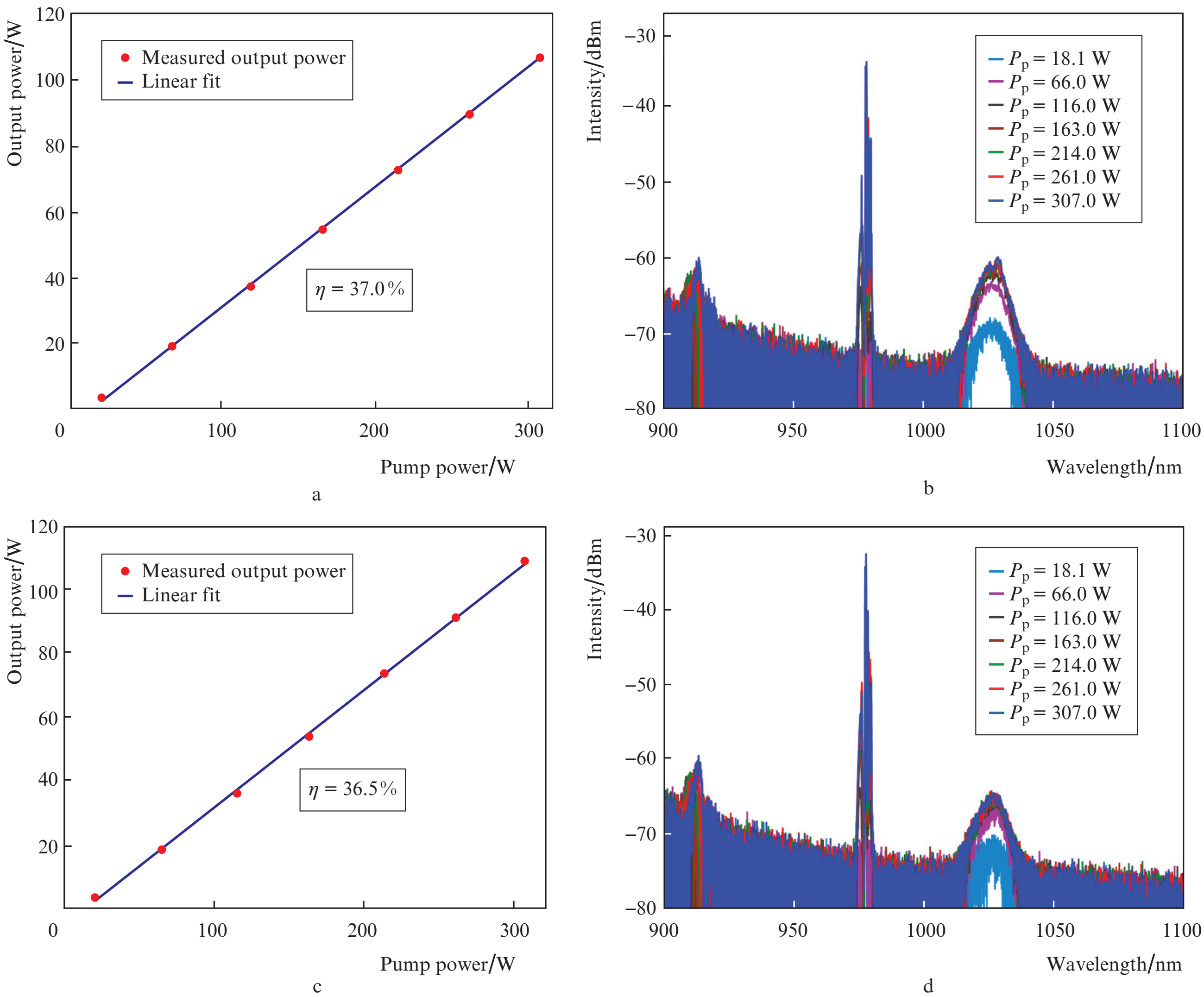

Figure 4. (Colour online) Dependences of the measured output power, slope efficiency and spectrum on the pump power with the 1.3-m (a, b) and 1.2-m (c, d) length active fibre.

However, the measured spectra (see Fig. 3b and Figs 4b and 4d) show that the output power does not only contain the signal light around 980 nm, but also contains the 1030-nm ASE. It can be seen that the 1030-nm ASE should decrease with shortening active fibre, but it is still a question how the signal power around 980 nm will vary with the active fibre length. In order to answer this question, we estimated the output powers of the 980-nm signal light by integrating the output spectrum. The pertinent results are given in Fig. 5a.

From Fig. 5a, it is a little unexpected to find that the slope efficiency of the 980-nm output power increases, rather than decreases, with shortening active fibre length, which is different to the results of the measured output power given in Fig. 3a and Figs 4a and 4c. The maximum 980-nm output power is obtained with the 1.2-m active fibre. In order to reveal the reason, we estimated the output power of 1030-nm ASE (Fig. 5b). It can be seen from Fig. 5b that with the 1.4-m active fibre, although 21.5-dB peak-to-peak suppression is realised at a maximum output power (see Fig. 3b), the output 1030-nm ASE can reach to 15 W because of its broad band. It means that the 1030-nm ASE should take 13.2% of the measured output power, without which the slope efficiency will decrease. Figure 5b also shows that even with the 1.3-m active fibre (25.8 dB peak-to-peak suppression of 1030-nm ASE), about 6.76-W 1030-nm ASE can still be coupled out at a maximum pump power which takes 6.07% of the total power. Only when the active fibre is shortened to 1.2 m, the ASE can be lowered to 2.3 W (about 2.1% of the total power). It means that because of the relatively strong ASE, the 980-nm output power is lowered with the active fibre lengthened from 1.2 m to 1.4 m, although the pump absorption and total output power are enlarged. It is also implied that the effect of 1030-nm ASE should not be negligible when its peak-to-peak suppression is lower than 30 dB.

Considering that the 1030-nm ASE is only 2.1% of the total power with the 1.2-m active fibre and its further suppression will help very little to improve the output power, we took this length as an optimum length of active fibre. With such length, about 105.6-W 980-nm output power is obtained with the slope efficiency about 35.8%. The above results also imply that corresponding to the optimum length of active fibre, the peak-to-peak suppression of 1030-nm ASE should not be smaller than 30 dB, which is also coincident with the numerical results given in Ref. [25] (see Fig. 2 in paper [25]).

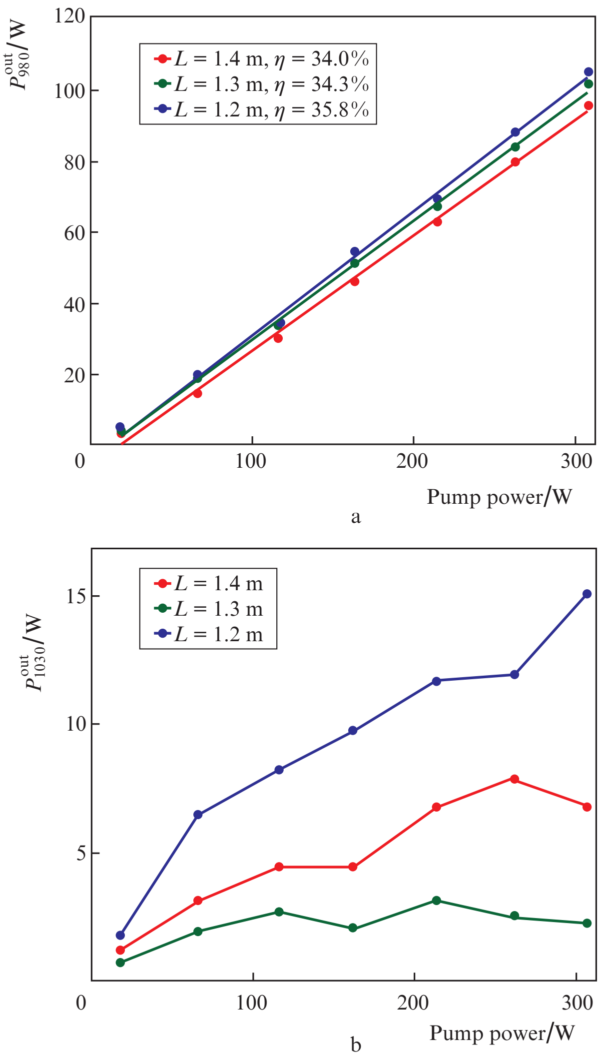

Figure 5. (Colour online) Dependences of the estimated output power at a wavelength of (a) 980 and (b) 1030 nm on the pump power at different active fibre lengths L.

3.2. Effect of the seed power

Besides the length of the active fibre, we also studied the effect of the seed power on the amplifier by using an optimum active fibre length of 1.2 m and varying the seed power from 3 W to 14 W. The measured output powers at different seed powers are shown in Fig. 6a. It can be seen that the output power and the slope efficiency increase monotonically with the seed power when the seed power is less than 9 W. However, it can also be seen that although the output power still increases with the increment of the seed power, the slope efficiency keeps around 36.5% when the seed power is over 9 W. In order to further illustrate the effect of the seed power on the amplifier, the added powers (output power minus seed power) with various seed powers are also given in Fig. 6b. It can be found that the slope efficiency is not varied when the added power is used instead of the output power, and the slope efficiency is increased by enlarging the seed power, which implies that a larger seed power is indeed beneficial to the amplification of the signal light near 980 nm because of better gain competition with the 1030-nm ASE.

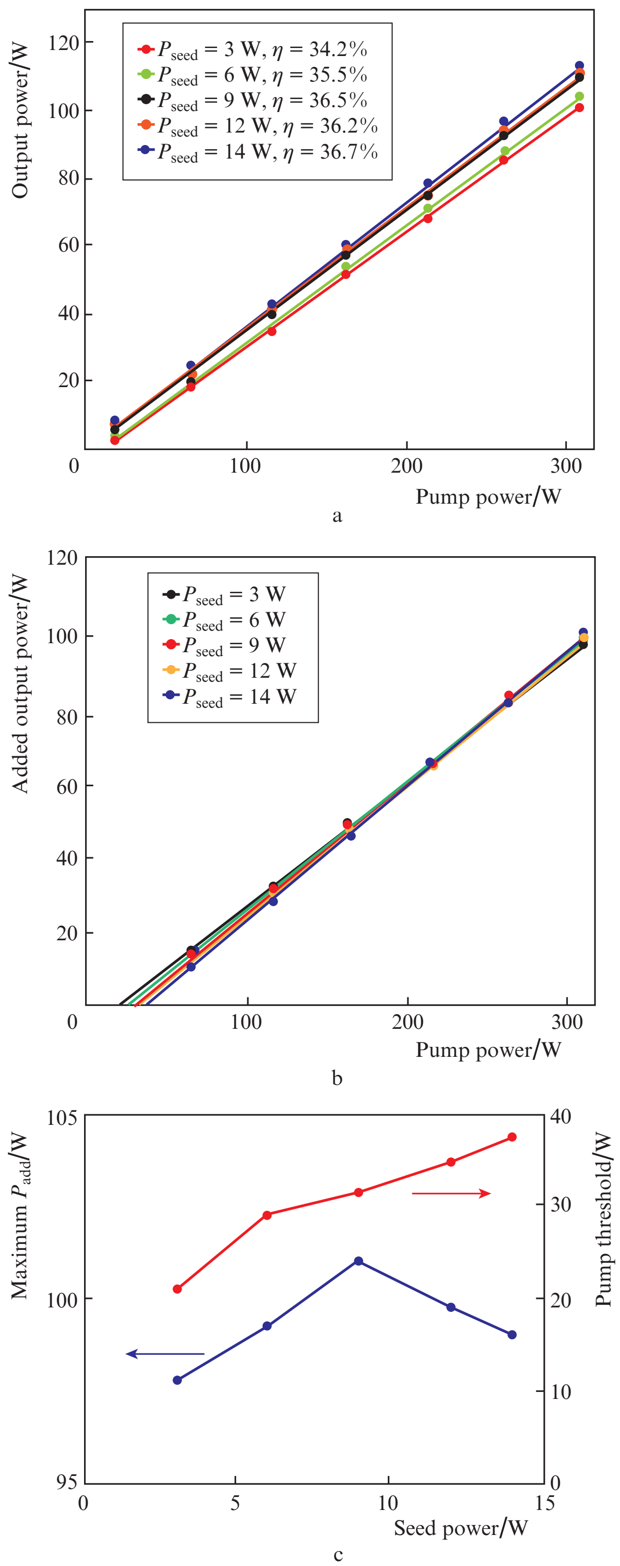

Figure 6. (Colour online) Dependences of (a) the output power and (b) added output power P_{add} on the pump power at various seed powers P_{seed}, as well as (c) dependences of the maximum added output power and pump threshold on the seed power.

In spite of that, by calculating the added power, it is also found that the maximum added power is obtained with the 9-W seed power when the pump power is 307 W (see Fig. 6c). It can be seen that the pump threshold becomes larger with the larger seed power, which means that more pump light is needed for the transparent transmission of stronger seed light. Then, with the same pump power, the pump light used for the signal light amplification becomes less because of the higher pump threshold. Then, with the seed larger than 9 W, the added power becomes less with even the larger slope efficiency. However, it can be expected that with further increasing the pump power, the added power with the 14-W seed power will eventually become the largest.

Besides, we also estimated the output powers of the 980-nm signal light (Fig. 7). It can be found that the variation of slope efficiency of 980-nm output power is similar to the case of the total power (see Fig. 6a), which shows again that the seed power should not be too small for improving the slope efficiency. This result is quite expected because more 1030-nm ASE will be induced with a weaker seed power which will lower the output efficiency (noting that the ASE is bi-directionally propagating and only a portion of ASE can be exported from the output port). However, the output efficiency with the 14-W seed power is slightly lower than that with the 9-W seed power, which is caused by the worse suppression of 1030-nm ASE (see Fig. 8b). In spite of that, Fig. 7 also shows that the larger output power can be obtained with the larger seed power. With the 14-W seed power, the maximum output signal power around 980 nm is about 108.2 W.

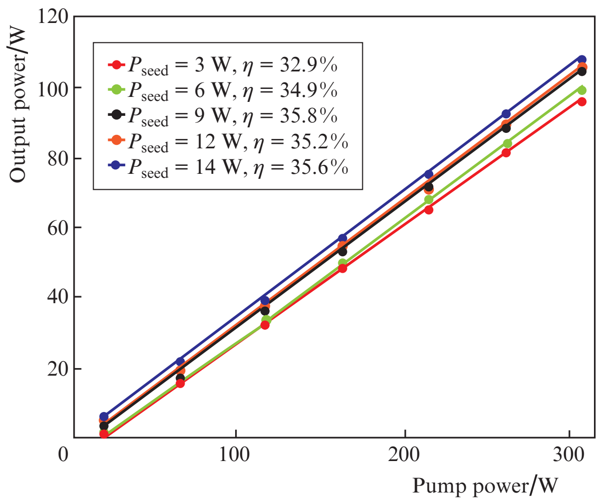

Figure 7. (Colour online) Estimated dependences of the 980-nm output power on various seed powers P_{seed}.

We also measured the output spectra at a maximum pump power of 307 W with various seed powers (Fig. 8a). To illustrate the dependence of 1030-nm ASE suppression on the seed power P_{seed}, we calculated the ratios of 1030-nm ASE power to the total and added 980-nm power at the maximum pump power (see Fig. 8b). It can help explain the variation of the slope efficiency given in Fig. 7, i.e., the higher slope efficiency should result from the better suppression of 1030-nm ASE (corresponding to the lower ratio of 1030-nm ASE). However, it can also be found that the best suppression of 1030-nm ASE is present with the 9-W seed power, rather than the 14-W seed power, which corresponds to the largest slope efficiency. The worse suppression of 1030-nm ASE with the 14-W seed power should also be induced by the larger pump threshold, which lowers the pump power used for signal amplifier (compared with the case of the 9-W seed power). It should be noted that the suppression of 1030-nm ASE should become better with increasing pump power. Then, the suppression of 1030-nm ASE with the 14-W seed power is slightly worse than that with the 9-W seed power.

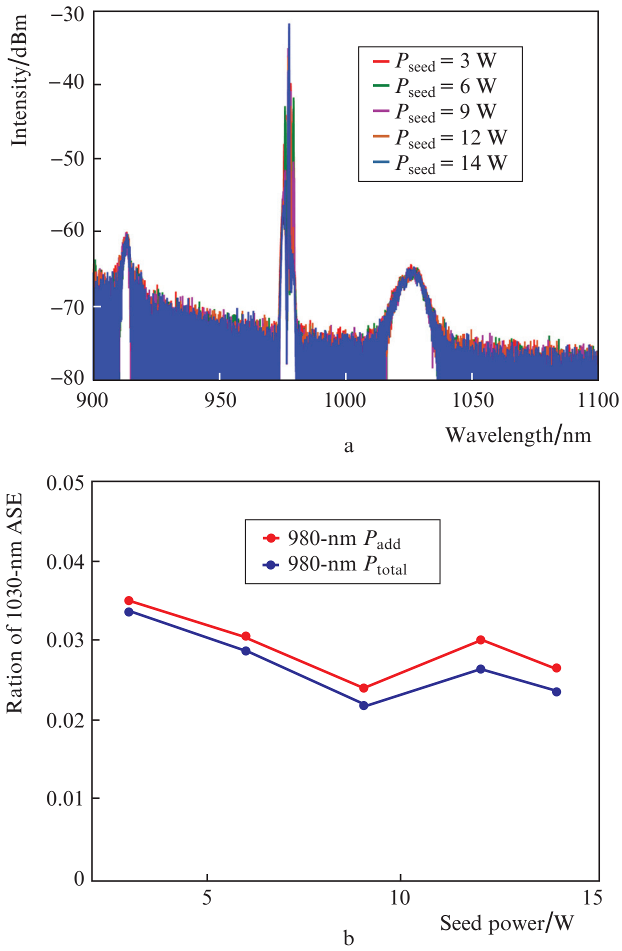

Figure 8. (Colour online) (a) Output spectra and (b) ratios of 1030-nm ASE to the total (P_{total}) and added (P_{add}) 980-nm power at various seed powers P_{seed} for the 307-W pump power.

4. Conclusions

We have experimentally demonstrated a 100-W all-fibre amplifier operating near 980 nm with a 60/125-µm core/cladding-diameter DCYF. With the 1.4-m active fibre, the 113.4-W output power is eventually obtained with the 9-W seed power. The slope efficiency is 38%, which is lower than the efficiency reported in Ref. [22] with the 60/140-µm DCYF (more than 45%). One possible reason is the relatively high pump loss due to the imperfection of outer-cladding coating and the not-so-well pump mixture induced by the octagon inner-cladding compared with the square inner-cladding used in Ref. [22]. Besides, by studying the effects of the active fibre length, we have found that although longer active fibre length is beneficial to the pump absorption, the 980-nm output power may be lower because of the stronger 1030-nm ASE. By estimating the output power of the 980-nm signal light and 1030-nm ASE with the spectral integration, we have revealed that the largest 980-nm output power (estimated about 105.6 W) can be obtained with the 1.2-m active fibre. We have also demonstrated that the 1030-nm ASE should not be negligible when its peak-to-peak suppression is lower than 30 dB.

The effect of the seed power has also been investigated. We have found that the seed power should be large enough (e.g., larger than 9 W in our experiment) for suppressing the 1030-nm ASE and improving the output efficiency. Then, with the 14-W seed power, about 108.2-W output signal power around 980 nm is eventually obtained. The power scalability of the 980-nm amplifier is limited by the pump power. The pertinent results can be of great guidance for the design and study of the 980-nm laser and other types of three-level fibre laser.

Acknowledgements. J. Cao would like to thank the 23th Research Institute of China Electronics Technology Group Corporation for useful help in fabricating the DCYF fibre and Zilun Chen, Peng Liu and Xiaolin Wang for their help in the experimental study.

References

1. Richardson D.J., Nilsson J., Clarkson W.A. *J. Opt. Soc. Am. B*, **27** (11), 63 (2010).
2. Kurkov A.S. *Laser Phys. Lett*., **4** (2), 93 (2007).
3. Cao J., Guo S., Xu X., Chen J., Lu Q. *IEEE J. Sel. Top. Quantum Electron*., **20** (5), 373 (2014).
4. Soh D.B.S., Codemard C., Wang S. *IEEE Photonics Technol. Lett*., **16** (4), 1032 (2004).
5. Li P., Zhong G., Liu Z., Chi J., Zhang X., Yang C., Zhao Z., Li Y., Wang X., Zhao H., Jiang D. *Opt. Laser Technol*., **44** (7), 2202 (2012).
6. Laroche M., Bartolacci C., Cadier B., Gilles H., Girard S., Lablonde L., Robin T. *Opt. Lett*., **36**, 3909 (2011).
7. Jelger P., Engholm M., Norin L., et al. *J. Opt. Soc. Am. B*, **27** (2), 338 (2010).
8. Paschotta R., Nilsson J., Tropper A.C., Hanna D.C. *IEEE J. Quantum Electron*., **33**, 1049 (1997).
9. Nilsson J., Minelly J.D., Paschotta R., Tropper A.C., Hanna D.C. *Opt. Lett*., **23** (5), 355 (1998).
10. Liu Y., Cao J., Xiao H., Guo S., Si L., Huang L. *J. Opt. Soc. Am. B*, **30** (2), 266 (2013).
11. Wang R., Liu Y., Cao J., Guo S., Si L., Chen J. *Appl. Opt*., **52**, 5920 (2013).
12. Selvas R., Sahu J.K., Fu L.B., Jang J.N., Nilsson J., Grudinin A.B., Ylä-Jarkko K.H., Alam S.A., Turner P.W., Moore J. *Opt. Lett*., **28** (13), 1093 (2003).
13. Röser F., Jauregui C., Limpert J., Tünnermann A. *Opt. Express*, **16** (22), 17310 (2008).
14. Boullet J., Zaouter Y., Desmarchelier R. *Opt. Express*, **16** (22), 17891 (2008).
15. Leich M., Jäger M., Grimm S., Hoh D., Jetschke S., Becker M., Hartung A., Bartelt H. *Laser Phys. Lett*., **11** (4), 045102 (2014).
16. Aleshkina S.S., Levchenko A.E., Likhachev M.E. *IEEE Photonics Technol. Lett*., **30** (1), 127 (2018).
17. Pureur V., Bigot L., Bouwmans G., Quiquempois Y., Douay M., Jaouen Y. *Appl. Phys. Lett*., **92** (6), 061113 (2008).
18. Matniyaz T., Kalichevsky-Dong M.T., Hawkins T.W., Parsons J., Gu G., Li W., Faykus M., Selee B., Dong J.A., Dong L. *Proc. 2018 OSA Laser Congress* (ASSL) (Boston, MA, 2018) paper AM6A.28. DOI:10.1364/ASSL.2018.AM6A.28.
19. Matniyaz T., Kalichevsky-Dong M.T., Hawkins T.W., Parsons J., Gu G., Li W., Faykus M., Selee B., Dong J.A., Dong L. *Proc. SPIE*, **10897**, 108970V (2019).
20. Matniyaz T., Li W., Kalichevsky-Dong M., Hawkins T.W., Parsons J., Gu G., Dong L. *Opt. Lett*., **44**, 807 (2019).
21. Li W., Matniyaz T., Kalichevsky-Don M.T., Gafsi S., Hawkins T.W., Parsons J., Gu G., Dong L. *Opt. Express*, **27**, 24974 (2019).
22. Aleshkina S.S., Bardina T.L., Lipatov D.S., Bobkov K.K., Bubnov M.M., Gur'yanov A.N., Likhachev M.E. *Quantum Electron*., **47** (12), 1109 (2017) [*Kvantovaya Elektron*., **47** (12), 1109 (2017)].
23. Valero N., Feral C., Lhermite J., Lhermite J., Petit S., Royon R., BardinY.V., Goeppner M., Dixneuf C., Guiraud G., Proulx A., Taillon Y., Cormier E. *Opt. Lett*., **45** (6), 1495 (2020).
24. Ren Y., Cao J., Chen H., Ying H., Pan Z., Du S., Chen J. *Opt. Express*, **26** (14), 17830 (2018).
25. Ren Y., Cao J., Du S., Chen J. *Optik,* **161**, 118 (2018).
26. Chen M., Li Z., Cao J., Liu A., Huang Z., Chen J. *Optik*, **228** (2021). DOI: 10.1016/j.ijleo.2020.166131.